ELSEVIER

Ceramics International 29 (2003) 777–784

CERAMICS INTERNATIONAL

www.elsevier.com/locate/ceramint

Fracture toughness of ceramics and ceramic composites

George A. Gogotsi

Institute for Problems of Strength, 2 Timiryazevskaya Street, Kiev 01014, Ukraine

Received 22 July 2002; received in revised form 9 September 2002; accepted 10 November 2002

Abstract

The fracture toughness of zirconia, alumina, and silicon nitride ceramics, zirconia and alumina single crystals, silicon carbide as well as silicon nitride ceramic particulate composites, silicon nitride laminated composites, and other ceramics materials were studied by a single edge V-notched beam (SEVNB) method. Manual and mechanical procedures for V-notch polishing-out and three- and four-point flexure tests were developed. Load–deflection diagrams for V-notched specimens contributed to better understanding of the deformation behavior of ceramics at room temperature and 1300–1400 °C. SENB (single edge notched beam) and SEPB (single edge precracked beam) as well as micro-Raman spectroscopy data were used to analyze the SEVPB results. The ratio between SEVNB and SENB results is about 0.6 for elastic materials, over 0.9 for inelastic ones, and about 1.0 for laminated ceramic composite. The polishing-out of a V-notch does not lead to the tetragonal-monoclinic phase transformation in zirconia ceramics.

Keywords: B. Composites; B. Spectroscopy; C. Fracture; C. Toughness; Ceramics; SEVNB-method

1. Introduction

Ceramics and ceramic composites are promising materials having rather high strength characteristics but quite low crack resistance properties at the same time. This is one of the major factors hindering the wide-scale application of these materials in various fields of human activities. The crack resistance is critical not only for ceramic products operating under extreme mechanical and thermal loads but also for structural components whose brittle fracture is intolerable even under arbitrary loads.

For many years, the performance of ceramics has been evaluated on the basis of full-scale tests. However, their fracture toughness characteristics have not always been the object of scientific interest. Wide-scale fracture toughness investigations were started only in the late 1980s. International prestandard studies (Round Robin on Fracture Toughness–RRFT [1]) aimed at the assessment of the accuracy and reliability of the data obtained by commonly accepted test methods were important steps in this field. Leading specialists from different countries engaged in those investigations performed statistical analyses to compare the test methods summarized in Table 1. They were helpful for creating the basis of more reliable determination of the fracture toughness characteristics of ceramics. For a long time, no particular preference was given to any of the methods considered because each of them had appreciable shortcomings, which restricted their application [2,3]. Recently, much attention has been focused on the SEVNB method [4], which is a further development of a simple and widely used the single edge notched beam (SENB) method suitable only for rough fracture toughness evaluations. The test data obtained by the SEVNB method were found to be comparable to those obtained by the single edge precracked beam (SEPB) method usually considered as providing the real values of critical stress intensity factor (K_{Ic}) but this test is often difficult to realize in practice [5]. To evaluate the potentials of the SEVNB method as a standard one for testing ceramics, its analysis was performed [6]. We verified the efficiency of our procedures and demonstrated the applicability of the SEVNB method to different ceramic materials.

E-mail address: ggogotsi@ipp.adam.kiev.ua (G.A. Gogotsi).

0272-8842/03/$30.00 © 2003 Elsevier Ltd and Techna S.r.l. All rights reserved.
doi:10.1016/S0272-8842(02)00230-4

2. Experimental

2.1. Materials

Isostatically pressed silicon nitride ceramics (Si_3N_4) [7], sintered (Y-PSZ) [8] and sintered under pressure (Y-PSZa) partially-stabilized zirconia ceramics [9] were the major materials used in the process of verifying the experimental procedures. Gas-pressure sintered silicon nitride (GPSSN) as well as sintered alumina (Al_2O_3-998) and silicon carbide (SSiC) [6] analyzed in the RRFT'97 also became the objects of the investigation. In our experiments we also used zirconia and alumina single crystals as well as silicon nitride based laminated composites with compressed Si_3N_4 and tensile-stressed Si_3N_4 + n wt.% TiN layers [10]. This composite, layers of which were prepared by rolling, was produced by hot pressing at 1850 °C for 20 min under pressure 150 MPa. For high-temperature investigations, reaction-bonded and sintered Si_3N_4 + 30% SiC + 3% MgO [11] and hot-pressed (in graphite molds) SiC + 50%ZrB_2 + 10% B_4C [12] ceramic particulate composites were also used. Some data on these ceramics are given in Table 2.

2.2. Test specimens

Rectangular beams (3 mm×4 mm cross-section) V-notched in two stages were used as test specimens [7]. The package of 2–6 specimens were glued onto a ceramic plate and then V-notched. Two additional specimens were fixed on both sides of the package for its protection from the edge effects due to notching. A preliminary notch 0.8 mm deep (specimens for four-point flexure) or 1.6 mm deep (specimens for three-point flexure) was cut in the package by a 150–300 μm thick diamond disk. At the next stage, the V-notch was manually (convenient for comparatively "soft" ceramics) or mechanically (necessary for "hard" ceramics) polished-out after filling the preliminary notch with a diamond paste of grain sizes ranging from 2 to 7 μm and a razor blade 150–300 μm thick. In the case of manual polishing-out, the walls of the preliminary notch (1.6 mm deep) served as the razor blade guides. The purpose of the test determined the number of notches (one or three) cut in a standard 45-mm long specimen (Fig. 1). The criterion for the proper V-notch sharpness is its width, S, equal to two root radii ρ. The notch

Table 1
Conventional ceramics fracture toughness test methods

Specimen	Method and fracture surface of specimen	Specimen	Method and fracture surface of specimen
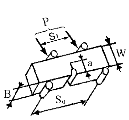	SEPB  (single edge precracked beam)	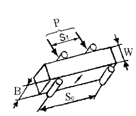	SCF 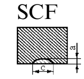 (surface crack in flexure)
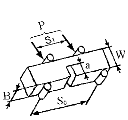	SENB  (single edge notched beam)	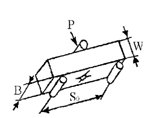	IS 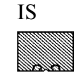 (indentation strength)
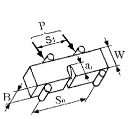	CNB 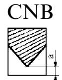 (chevron notched beam)	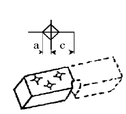	IF (indentation fracture)

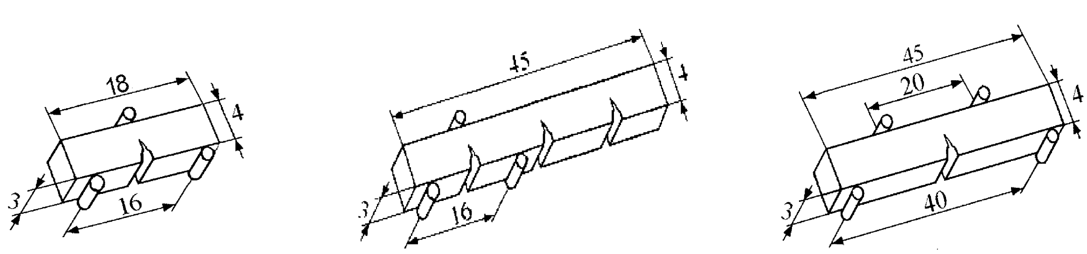

Fig. 1. SEVNB specimens: a, b, three-point flexure; c, four-point flexure.

length and radius were measured with optical (Olimpus BX51M) and scanning electron microscopes (×500 or better).

2.3. Procedures

The specimens were tested in three-point (16 mm span between the bearing rollers) or four-point flexure (20–40 mm spans between the bearing rollers) on a home-made Ceramtest block, mounted on a universal testing machine and fitted with a hard load cell, a system for precision displacement of a loading rod, and loading supports. The latter are equipped with an attachment for the rotation of the bearing rollers during specimen loading. Three-point flexure required the precise alignment of a specimen on the bearing rollers, with the axis of the central bearing roller and the radius of the V-notch root being in the same plane as the applied load. In high-temperature tests, we used a loading block which is similar to that used in room temperature tests.

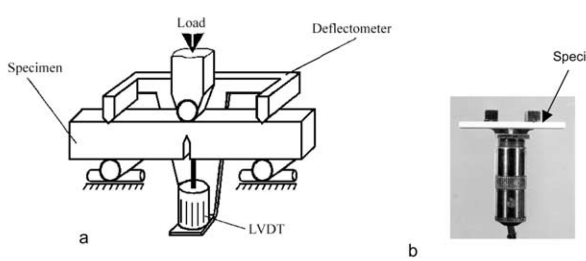

Fig. 2. Loading scheme for three-point flexure (a) and deflectometer suspended on a specimen 3×4×45 mm^3 (b).

For the recording of the load–deflection curves, a high-sensitivity LVDT-based deflectometer was suspended on a specimen (Fig. 2) and was in no way connected to the testing arrangement [13]. The LVDT was located outside the heating chamber in case of high-temperature tests.

In all the experiments, the speed of the testing machine crosshead was constant and equal to 0.5 mm/min. Load cell and deflectometer readings were recorded with a coordinate potentiometer.

Fracture toughness, K_{Ic} values were calculated in accordance with ASTM standard [14] (three-point flexure tests) and DIN one [15] (four-point flexure tests). Additional procedures for evaluating K_{Ic} and other mechanical characteristics are described elsewhere [16].

A micro-Raman imaging microscope (Renishaw, USA) with a 514.5 nm excitation line of an argon laser (×100 objective and a ~1-μm diameter spot) was used to examine the surfaces of fractured Y-PSZ specimens by a procedure described in Ref. [17].

3. Results and discussion

The results of comparative three- and four-point flexure tests of monolithic ceramics and particular ceramic composites are summarized in Table 3, where the data obtained within the RRFT'97 program are also cited. The variation of K_{Ic} values as a function of notch root radius was studied for silicon nitride and zirconia (Fig. 3). Load–deflection diagrams for V-notched specimens are

Table 2
Characteristics of some materials

Material	Density (g/cm^3)	Strength at 20 °C (MPa)	Hardness (GPa)	Method of manufacture
Si_3N_4	3.14	700	14.1	HIP
GPSSN	3.23	>920	13.5	Gas-pressure sintered[a]
SSiC	3.15	–	22.4	Sintered[a]
Al_2O_3-998	3.86	350	19.3	Sintered[a]
Y-PSZ	6.05	425	12.1	IP + sintered

[a] Material of RRTF'97.

Table 3
Comparative fracture toughness tests (MPa m$^{1/2}$)

Test method	Three-point flexure (a/W≈0.5)	Four-point flexure (a/W≈0.2...0.3)	
		Our results	RRFT'97 results
Si_3N_4	5.5±0.07 (5)[a]	5.35±0.16 (5)	–
GPSSN	5.3±0.04 (5)	5.2±0.18 (5)	5.36±0.34 (129)
Si_3N_4+30%SiC+3% MgO	2.27±0.14 (4)	2.40±0.16 (5)	–
SSiC	2.45 (1)	2.66±0.20 (4)	2.61±0.18 (56)
SiC+50%ZrB_2+10% B_4C	3.59±0.12 (3)	3.51±0.15 (3)	–
Al_2O_3-998	3.5±0.05 (5)	3.6±0.06 (5)	3.57±0.22 (135)
Y-PSZ	5.7±0.17 (5)	5.9±0.19 (5)	–

± Standard deviation.
[a] The number of specimen tested (in parentheses).

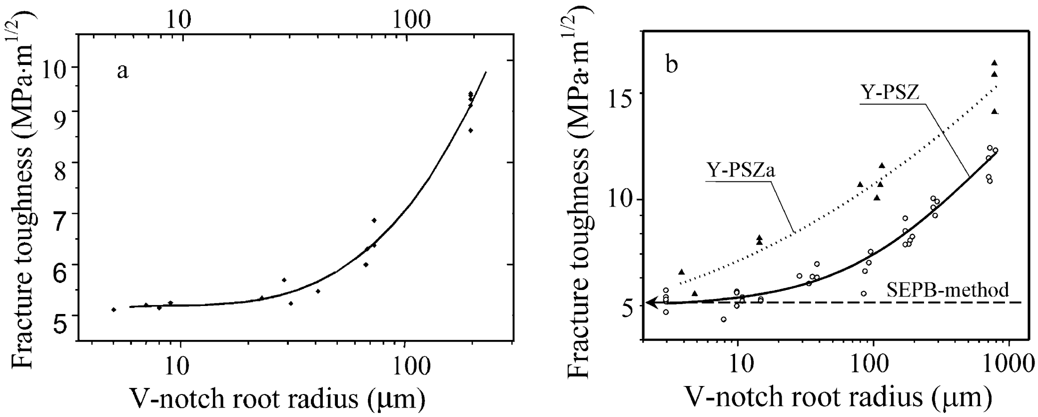

Fig. 3. Effect of V-notch root radii on the K_{Ic} values for Si_3N_4 (a) and Y-PSZ (b) ceramics.

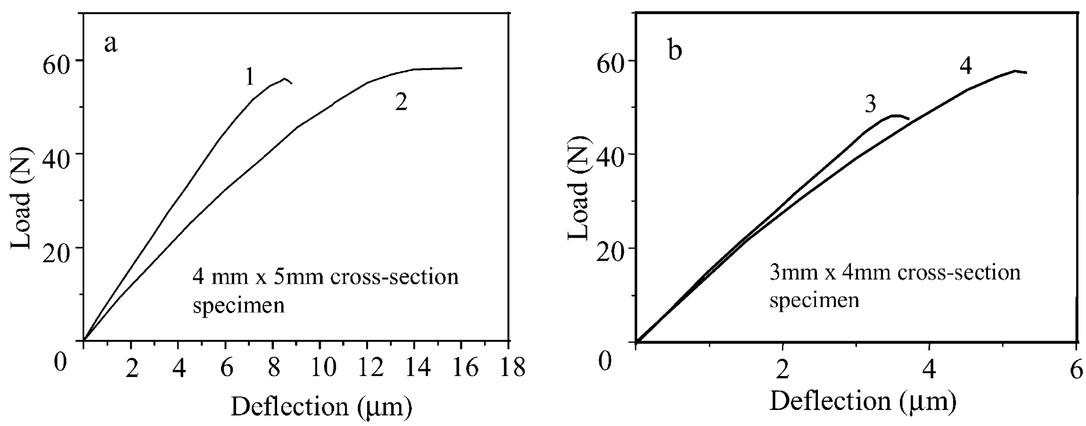

Fig. 4. Load–deflection diagrams for notched Si_3N_4 + 30% SiC + 3% MgO (a) and SiC + 50% ZrB_2 + 10% B_4C (b) specimens tested at room temperature (1, 3) and at 1400 °C (2, 4).

presented in Figs. 4 and 5. The results of micro-Raman analysis are given in Fig. 6. The comparative data on SEVNB and SENB results are summarized in Tables 4–6. High-temperature test results are cited in Table 7.

It is useful to start the analysis with emphasis on the K_{Ic} values obtained in three- and four-point flexure (Table 3). The data presented in this table demonstrate good agreement between our results and the average results of RRFT'97 [6], which confirms sufficient accuracy of our test procedures. The comparison of the data presented in Table 3 also points to the fact that essential differences between three- and four-point flexure results are absent. A similar conclusion was also made elsewhere [18] for ceramic matrix composites. Consequently, both test methods might be considered identical. Moreover, four-point flexure can be more easily applied in practice because it does not require a precise placement of specimens on the bearing rollers, which is difficult to achieve without a trained operator. On the other hand, three-point flexure tests can utilize small-size specimens, which is advantageous for materials science research.

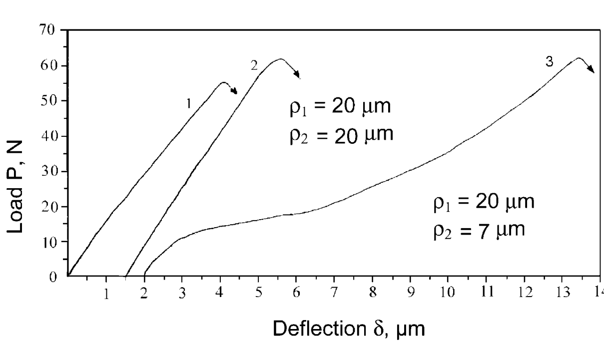

Fig. 5. Load–deflection diagrams for notched SiC + 50%-TiB_2 + 10%B_4C specimens with V-notch root radiuses ρ_1 and $\rho 2$ are equal (1 and 2) and differed (3) in values on them opposite sides.

The analysis of results (Fig. 3) shows that a decrease in the V-notch radius of a specimen leads to an essential decrease in the K_{Ic} values for Si_3N_4 and Y-PSZ ceramics (similar relation was also observed for other materials [2]). It is interesting to note that the fracture toughness-notch root radius curve for Si_3N_4 (Fig. 3a) flattens in the vicinity of a small notch root radius as compared to that of the Y-PSZ (Fig. 3b). Such an effect is probably determined by different sensitivity of these materials to stress concentrations because of differences in their grain sizes (~4 μm for Si_3N_4 and >1 μm for Y-PSZ) as it was mentioned elsewhere [19]. It should be emphasized that only for notch root radii less than 5–7 μm [7] the K_{Ic} values for Y-PSZ ceramics agree with SEPB data (similar behavior is also typical of fine-grained alumina [20]. A similar conclusion follows from [6], where an attempt was made to relate the V-notch radius values required for the correct determination of K_{Ic} values to the averaged values of this parameter obtained in the RRFT'97 studies. As follows from Fig. 3a, the decrease in K_{Ic} values for Si_3N_4 ceramics occurs with a decrease in notch radii down to about 30 μm, which does not contradict the results of sintered SiC whisker-reinforced Si_3N_4 [18] tests. A similar tendency is also typical of SiC ceramics [19].

The examination of the specimens fractured in the tests revealed a fracture crack that propagated from the points where "additional" stress concentrators were present. This observation also confirms the assumption that the fracture of a loaded ceramic specimen starts from a small crack ahead of a machined notch root [19]. In this context, it is interesting to mention that K_{Ic} magnitudes are influenced by the sharpness of a notch root rather than by its shape [7].

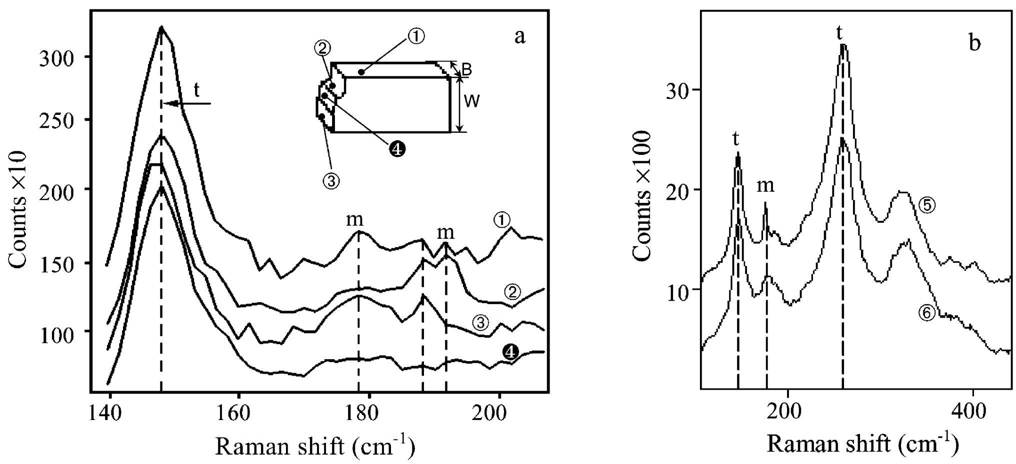

Fig. 6. Raman spectra of Y-PSZ specimens fractured by the SEVNB method (a) and by indentation (b): nonfractured specimen surface (1), diamond saw surface (2), fracture surface (3), razor blade surface (4), indentation edge (5), and indentation center (6).

Table 4
K_{Ic} values for ceramics obtained by SEVNB and SENB methods (MPa $m^{1/2}$)

Material	Test method		Flexure (points)	Index φ	Brittleness measure, χ
	SEVNB	SENB[a]			
Y-PSZ	5.14±0.29	9.54±0.47	Four	0.538	1
Soda limit glass	0.66±0.07	1.18±0.09	Four	0.562	1
$SiC+50\%ZrB_2+10\%B_4C$	3.52±0.08	6.24±0.37	Three	0.564	1
Si_3N_4	5.17±0.06	9.12±0.29	Three	0.567	1
SSiC	2.61±0.18	4.42±0.23	Four	0.590	1
$Si_3N_4+30\%SiC+3\%MgO$	2.27±0.14	2.49±0.16	Three	0.920	0.88
Mg-PSZ (TS-grade)	9.44±0.12	10.2±0.27	Four	0.925	0.41
$La_{8.8}Ca_{0.2}CoO_3$	2.2	2.2	Three	1	0.25

[a] The width of notch is 0.2–0.3 mm.

Table 5
K_{Ic} values for single crystals obtained by SEVNB and SENB methods (MPa $m^{1/2}$)

Single crystals	Peculiarity	Elastic modulus (GPa)	Test method		Brittleness measure, χ	Index φ
			SENB	SEVNB		
Zirconia	Partially stabilized (3% Y_2O_3)	245	9.33±0.95	10.33±2.17	1	0.9
Alumina	Specimen axis 45° to optical axis of crystal	403	2.31±0.34	2.45±0.29	1	0.94
	Specimen axis 90° to optical axis of crystal	410	3.19±0.53	2.85±0.50	1	1.12

Table 6
K_{Ic} values for Si_3N_4/Si_3N_4 + n% TiN laminated composites (χ = 1) obtained by SEVNB and SENB methods (MPa $m^{1/2}$)

Content (n) of TiN layers[a] (%)	Test method			Average value of K_{IC} (MPa $m^{1/2}$)
	SEVNB		SENB	
	Four-point flexure, 20/40 mm	Three-point flexure, 16 mm	Three-point flexure, 16 mm	
	K_{IC} (MPa $m^{1/2}$)	K_{IC} (MPa $m^{1/2}$)	K_{IC} (MPa $m^{1/2}$)	
10	6.61	6.80	6.27	6.56±0.19
	6.45	6.37	5.74	6.19±0.30
	5.95	6.20	6.08	6.08±0.08
	5.26	5.59	7.03	5.96±0.71
	5.42	5.48	8.41	6.43±1.32
	5.26	5.90	4.94	5.37±0.36
	6.45	6.03	6.01	6.16±0.19
	5.87	5.71	5.85	5.81±0.07
Average	5.91±0.46	6.01±0.36	5.99±0.41	
30	8.57	8.11	9.15	8.66±0.58
	9.84	9.31	9.28	9.48±0.24
	8.91	8.20	9.09	8.73±0.36
	9.63	7.87	8.07	8.52±0.74
Average	8.99±0.75	8.37±0.47	8.90±0.41	

[a] Average thickness of layers is 0, 185 mm.

The SEVNB method (see, e.g., [6]) is usually compared with the SEPB, SCF, and CNB methods. But it is also feasible to compare SEVNB and SENB data (Table 4), paying attention to the fact [21,22] that the evaluation of inelastic materials gives fracture toughness results which practically coincide with those for the specimens with sharp and blunt stress concentrators. Table 5 summarized the index of sensitivity to stress concentrations, φ, equal to the ratio of the K_{Ic} values obtained by the SEVNB and SENB methods, and the inelasticity of ceramics described by the brittleness measure χ [22]. The latter is equal to the ratio of the specific elastic energy accumulated in ceramics by the moment of fracture to the total energy spent for its deformation. Brittleness measure values were determined from stress–strain curves obtained in four-point flexure of solid (without stress concentrators) specimens. The analysis of these data confirms the existence of relationship between φ and χ. In the tests of elastic materials ($\chi = 1$), φ is about 0.6, and for inelastic materials ($\varphi < 1$), it exceeds 0.9. But this conclusion is correct only for monolith ceramics and ceramics particulate composites. For single crystals (Table 5) and ceramic laminated composites (Table 6) the picture is different and above-mentioned dependence is not observed.

Almost all the studies on the deformation behavior of V-notched ceramic specimens with a φ value of about 0.6, produced linear load-deflection diagrams or diagrams with small nonlinearity (e.g., curves 1 and 3 in Fig. 4), which is associated with a comparatively slow crack growth that is permissible in accordance with [23].

Table 7
High temperature fracture toughness test results (SEVNB method)

Materials	K_{IC} (MPa $m^{1/2}$)		
	20 °C	1300 °C	1400 °C
Si_3N_4	5.5±0.1	4.2±0.3	–
Si_3N_4+30%SiC+3%MgO	2.27±0.1	–	2.68±0.1
SiC+50%ZrB_2+10%B_4C	3.52±0.1	3.63±0.3	3.70±0.1
Si_3N_4 [17][a]	5.6±0.5	5.0±0.4	–

[a] The notches were produced by diamond saw with V-shaped tip.

But in some tests of ceramics particulate composites, the situation was different, especially if the sharpness of a V-notch was not uniform (V-notch root radii on the opposite sides of the specimen are not equal). Several load-deflection diagrams can have an unusual shape because fracture initiates in the vicinity of the notch root with a smaller radius, where higher stress concentrations are present (Fig. 5).

To complete the analysis of Table 4, we should note that in fracture toughness tests of TS-grade zirconia ceramics, the index φ was lower than unity. At the same time, the comparison of SENB and SEPB data for these ceramics (if the annealing of specimens was not performed at temperatures exceeding the boundary of monoclinic-tetragonal transformation) could give a ratio of K_{Ic} values more than unity. For example, this ratio was 1.24 [24], which was probably caused by the phase transformation in the area of the initial crack nucleation, when the specimen was prepared for SEPB. Therefore, it was interesting to investigate the phase state on the fracture surfaces of zirconia specimens tested by the SEVNB method. The phase state was analyzed by micro-Raman spectroscopy (Fig. 6), which demonstrates, in contrast to fracture or saw notch surfaces (Fig. 6a) or the edge of indentation (Fig. 6b), a polished V-notch surface does not contain the monoclinic phase (there is no effect inducing the phase transformation). This is an important advantage of the SEVNB method in comparison with other fracture toughness test methods for zirconia and similar ceramics.

The comparison of high-temperature K_{Ic} evaluations for Si_3N_4 ceramics, presented both in Table 7 and in Ref. [18], reveals their similarity. However, in our case, in contrast to [18], fracture of the V-notch surface did not occur and we did not observe active oxidation in the vicinity of the notch. It is noteworthy that in SEPB tests of similar ceramics [18], oxidation induced the blunting (healing) of the initial sharp crack and, as a consequence, the fracture toughness results varied.

It is necessary to emphasize the increase in the fracture toughness of ceramic particulate composites with test temperatures (Table 7). The φ value varies moderately with this increase (0.81 for Si_3N_4 + 30% SiC + 3% MgO and 0.71 for SiC + 50% ZrB_2 + 10% B_4C). The changes in the load-deflection diagrams of these ceramics with test temperatures are not so pronounced (Fig. 4) and are connected with a certain increase in their inelastic deformation. It should be noted that the load–deflection diagrams for Si_3N_4 + 30%SiC + 3% MgO unnotched specimens and specimens with wide notches were linear. The oxidation layers on fractured specimens are not strong and cannot affect the fracture toughness of the ceramics studied in high-temperature SEVNB tests. And, probably, the blunting of a stress concentrator does not occur as in [18], where in SEPB tests crack healing and a considerable increase in K_{Ic} values, even at 1200 °C, were observed.

4. Conclusions

The test data confirm that the SEVNB method can be easier applied in practice and can be used for the majority of advanced ceramics and ceramic particulate composites at different temperatures and in the oxidation environment. The SEVNB data for ceramics and ceramic particulate composites are independent of the flexure type and exhibit small scatter. For laminated ceramic composites them are also independent of width of the stress concentrator. Therefore it commands the attention of engineers involved in both certification testing and materials science research. It was found that the ratio between SEVNB and SENB data equaled about 0.6 for elastic ceramics and ceramics particulate composites and over 0.9 for inelastic ones. The polishing-out of a V-notch root does not damage the surface layer formed on a zirconia; therefore, there are no residual stresses, phase transformations or other effects, which often accompany the formation of stress concentrators by other procedures.

Acknowledgements

Thanks are expressed to Mr. V. Galenko and Mr. B. Ozersky (IPS, Ukraine) for their assistance in performing experiments. The investigation partially financed by INCO-Copernicus Grants (contracts 15 CT 96 07 29 and 1CA2-CT-2000-10020).

References

[1] G.A. Gogotsi, Fracture toughness studies on ceramics and ceramic particulate composites at different temperatures, in: J.A. Salem, G.D. Quinn, M.G. Jenkins (Eds.), Fracture Resistance Testing of Monolithic and Composite Brittle Materials (ASTM STP 1409), American Society for Testing and Materials, West Conshohocken, PA, 2002, pp. 199–212.
[2] J. Kübler, Fracture toughness of ceramics using the SEVNB method: preliminary results, in: J.P. Singh (Ed.), Ceramic Engineering & Science Proceedings, American Ceramic Society, Vol. 18, Issue 4, 1997, pp. 155–162.
[3] G.A. Gogotsi, V.I. Galenko, Comparative analysis of fracture toughness tests methods for ceramics and crystals at room and lower temperatures, Strength of Materials 29 (1997) 287–297.
[4] Le Bac, Verfahren zum Feinkerben von Keramischen Körpern, Patentschrift 146416, Deutsche Demokratische Republik- Amt für Efindungs- und Patentwesen, 1979–1981.
[5] D.J. Dameny, A. Danzer, Method for fracture toughness testing of ceramics—ready for standardisation, in: M.W. Brawn, E.R. Riosand, K.J. Miller (Eds.), Fracture from Defects, Emas Publishing, 1998, pp. 491–496.
[6] J. Kübler, Fracture Toughness of Ceramics Using the SEVNB Method: Round Robin, VAMAS Report No.37/ESIS Document D2-99, EMPA, Swiss Federal Laboratories for Materials Testing and Research, Dubendorf, Switzerland, 1999.
[7] G.A. Gogotsi, Fracture toughness of ceramics and ceramic matrix composites (SEVNB Method), Refractory and Technical Ceramics 11–12 (1998) 7–13.
[8] G.A. Gogotsi, Fracture toughness tests of V-notched specimens, Strength of Materials 32 (2000) 170–177.
[9] G.A. Gogotsi, V.I. Galenko, B.I. Ozerskiy, A.D. Vasiliev, V.I. Korban, Fracture resistance, strength, and other characteristics of Y-TZP, Refractory and Industrial Ceramics 8 (2000) 7–13 (in Russian).
[10] G.A. Gogotsi, M.I. Lugovy, V.N. Slyunyayev, N.A. Orlovskaya, Development of multilayered Si_3N_4-based ceramics composite having an ability to arrest cracks, Proc. of Int. Conf. Science for Materials 2002, IPMS, Kiev, 2002, pp. 247–248.
[11] G.A. Gogotsi, Several Experimental Results of High Performance Ceramics Used in Heat Engine Components, IPS AN USSR, Kiev, 1983 (in Russian).
[12] G.A. Gogotsi, Private communication.
[13] G.A. Gogotsi, V.P. Zavada, V.I. Nerodenko, USSR Patent No. 1 224 551, 15 December 1984.
[14] ASTM C1421-99, Standard Test Method for the Determination of Fracture Toughness of Advanced Ceramics at Ambient Temperature.
[15] Draft Standard DIN 51 109, Testing of Advanced Technical Ceramics; Determination of Fracture Toughness K_{Ic}, DIN NMP 291, September 1991.

[16] G.A. Gogotsi, Mechanical behaviour of yttria- and ferric oxide-doped zirconia in different temperatures, Ceramics International 24 (1998) 589–595.
[17] G.A. Gogotsi, E.E. Lomonova, Micro-Raman spectroscopy study of indentation-induced phase transformation in zirconia crystals, Refractory and Industrial Ceramics 41 (2000) 191–195.
[18] M. Mizuno, Y. Nagano, J.-W. Cao, J.-l. Kon, VAMAS round robin on fracture toughness measurements of ceramic matrix composite, in Abstracts, 9th International Conference on Modern Materials & Technologies (CIMTEC'98), Florence, Italy, June 1998, d. 108.
[19] R. Damani, R. Gstrain, R. Danzer, Critical notch-root radius effect in SENB-S fracture toughness testing, Journal of the European Ceramic Society 16 (1996) 695–702.
[20] T. Nishida, Y. Hanaki, G. Pezzotti, Effect of notch-root on the fracture toughness of a fine-grained alumina, Journal of the American Ceramic Society 77 (1994) 606–608.
[21] R.W. Davidge, G. Tappin, The effective surface energy of brittle materials, Journal of Materials Science 3 (1968) 165–173.
[22] G.A. Gogotsi, Deformational behaviour of ceramics, Journal of the European Ceramic Society 7 (1991) 87–92.
[23] ISO DIS 15 732. Fine Ceramic (Advanced Ceramics, Advanced Technical Ceramics)—Test Method for Fracture Toughness of Monolithic Ceramics at Room Temperature by Single Edge Precracked Beam (SEPB) Method, ISO/TC 206, 1999.
[24] G.A. Gogotsi, A.V. Drozdov, V.P. Zavada, M.V. Swain, Comparison of the mechanical behaviour of partially stabilised zirconia with yttria and magnesia, Journal of the Australian Ceramic Society 27 (1991) 37–49.